EUROPEAN ORGANIZATION FOR NUCLEAR RESEARCH

CERN-PPE/91-73
23 April 1991

Performance of a Liquid Argon Electromagnetic Calorimeter with an 'Accordion' Geometry

RD3 Collaboration

B.Aubert, A.Bazan, F.Cavanna, J.Colas, T.Leflour, J.P.Vialle
LAPP, Annecy, France

H.A.Gordon, V.Polychronakos, V.Radeka, D.Rahm, D.Stephani
Brookhaven National Laboratory, Upton, USA

L.Baisin, J.C.Berset, C.W.Fabjan,
D.Fournier*, O.Gildemeister, P.Jenni, M.Lefebvre†
C.P.Marin, M.Nessi, F.Nessi-Tedaldi, M.Pepe.
G.Polesello‡, W.Richter, A.Sigrist, W.J.Willis
CERN, Geneva, Switzerland

D.V.Camin, G.Costa, F.Gianotti, L.Mandelli, G.Pessina
Dipartimento di fisica dell'Universita e Sezione INFN, Milano, Italy

L.Iconomidou-Fayard, B.Merkel, P.Pétroff,
J.P.Repellin
LAL, Orsay, France

*also LAL, Orsay, France
†present adress: University of Victoria, Victoria, Canada
‡present adress: Sezione INFN, Pavia, Italy

Submitted to Nuclear Instruments and Methods

Abstract

The first prototype of a lead–liquid argon electromagnetic calorimeter with accordion–shaped absorber and electrode plates has been built and tested with electron and muon beams at the CERN SPS. This novel geometry combines good granularity with high readout speed and minimal dead space. For a response peaking time of 140 ns, an energy resolution of $10\%/\sqrt{\mathrm{E(GeV)}}$ and a space resolution of 4.4 $mm/\sqrt{\mathrm{E(GeV)}}$ with a 2.7 cm cell size have been achieved for electrons. The position accuracy for muons is better than 2 mm.

1 Introduction

Future high energy hadron colliders operating at high luminosity like LHC and SSC will set strong requirements for electromagnetic and hadronic calorimetry [1].

From past experience, both in fixed target and collider experiments, it is known that the liquid argon (LAr) technique provides, at reasonable cost, good energy resolution, good stability and accurate intercalibration of channels. It is also expected that this technique is intrinsically radiation resistant. Such properties, considered essential for operation at the future colliders, make a LAr based detector a potentially interesting candidate.

However, when operated as an ionization chamber in which all the negative charge from ionization is collected, such a detector is relatively slow, its response being driven by the electron drift time between the absorber and the electrode plate which is typically 400 ns for a 2 mm gap. A second limitation to fast readout comes from the long connections (several centimeters of cables in the best case) needed to interface the calorimeter cells to the electronic chain. Finally, no good solution had previously been found to read out a large barrel detector with high granularity (typically 2.5 $cm \times 2.5$ cm cell size), as needed at the LHC and SSC, without dead space between towers.

We present here a new approach, part of a recently started LHC R&D activity [2], in which the above–mentioned problems find, in principle, a satisfactory solution. In order to test this concept, a small electromagnetic calorimeter has been built and exposed to a high energy electron beam at the CERN Super Proton Synchrotron (SPS). Results on energy resolution, position resolution and uniformity of response are presented. Some results obtained with muons are also given.

This paper is organized as follows. Section 2 illustrates the principles on which this new detector is based while Section 3 describes in detail the test prototype. The test beam results obtained with electrons and muons are presented in Section 4. Finally Section 5 outlines some future prospects.

2 Fast Liquid Argon Calorimetry

One way to get a fast response from a LAr calorimeter is to exploit the very fast rise of the ionization current which is determined by the time (~ 1 ns) needed for an electromagnetic shower to develop inside the detector. In practice this can be done by integrating this current over an interval τ much shorter than the drift time t_d (Fig. 1a) using in the electronic chain a charge sensitive preamplifier followed by a bipolar shaper. Signal to noise ratio and peaking time of the response for such a configuration have been studied in detail in Ref. [3]. The peaking time $t_p(\delta)$ of the shaper response to a short current pulse (δ) becomes the characteristic time of the response instead of t_d, and it is approximately equal to the integration time. If no other time constant limits the response, the calorimeter signal has the shape depicted in Fig. 1c, and the signal to noise ratio scales as $t_p(\delta)^{3/2}$. In practice, however, the time constant τ_c of the circuit composed by the calorimeter cell capacitance, the connections to the preamplifier and the preamplifier input impedance can easily be longer than $t_p(\delta)$, thus deteriorating the signal to noise ratio.

In the scheme presented here, the time constant τ_c is small enough to allow pushing $t_p(\delta)$ to the order of 20 ns as required for operation at the LHC or SSC. However, during the short time available for the prototype construction fast shapers with such characteristics could not be developed and existing bipolar shapers with $t_p(\delta) \simeq 100$ ns, yielding an effective response time of 140 ns, had to be used instead. Beam tests with fast components are part of the forthcoming programme [2].

In a conventional LAr calorimeter one of the main contributions to τ_c comes from the capacitance and inductance due to the leads necessary to link together in a tower the small pads of successive planar parallel layers and from the connections to the preamplifier. In this new design the converter plates and the readout electrodes are no longer planar but have instead an accordion shape waving longitudinally, i.e. along the direction of the incident showering particle. In this way the connection of successive pads to form a tower is automatic when one cuts the readout electrodes into longitudinal strips. With preamplifiers mounted directly on each tower on the front and back faces of the calorimeter, the most favourable situation for reduced noise, maximum speed and low cross talk is achieved. This concept relies heavily upon adequate performances (low noise, low input impedance) of the readout preamplifiers which must work at LAr temperature. As described in Section 3.3 two different technologies for cold preamplifiers have been used with this prototype: Silicon J-FETs and Gallium Arsenide MESFETs.

The novel design allows also the assembly of a large detector in which dead spaces are to a great extent eliminated. This crucial aspect is discussed in Reference [2].

3 The Prototype Calorimeter

A module with 40 cm × 40 cm transverse section and with a depth of about 25 radiation lengths has been built to study electron showers at CERN SPS energies with full shower containment.

The converter plates are 1.8 mm Pb sheets (99.9% purity) clad in 0.1 mm of stainless steel. The readout electrodes are made of copper–clad polyimide "Kapton" [1] foils. Both the absorber and the readout plates are vertical and have an accordion shape with a pitch of 40.1 mm and an inclination angle of $\pm 45^0$ with respect to the nominal direction of incidence (Fig. 2). The LAr gap is 1.9 mm on either side of each electrode.

The Pb plates are held in place using an horizontal support in which accordion shaped grooves are machined. When all plates are in place a set of bars with similar grooves are installed on top as a cover. Two vertical side plates complete the box in which the detector was assembled (Fig. 3). Brass was chosen as the material for this support frame as its thermal expansion coefficient is close to that measured for the converter plates (0.30% of relative contraction when going from room to liquid nitrogen temperature). No attempt at all was made for this first prototype to minimize external support structures.

The Kapton plates are maintained in place between two adjacent converter plates using vertical bands of a light honeycomb structure [2]. At the front and the back

[1] Fortin industries. Sylmar, California.

[2] Type ECA from Eurom Composites SA.

ends each Kapton board is screwed to the converter plate to its left. This serves both as a mechanical fixation and as an electrical ground connection.

A potential source of non uniformity in the response of such a detector is the variation of the material density traversed by a particle as a function of its impact position along the horizontal direction x [3] In designing the prototype great importance was given to the understanding of this problem, and the amount of radiation lengths traversed both by minimum ionizing and by showering particles was extensively studied through simulations. Uniform response could be obtained if the detector plates had acute corners. With rounded corners, as needed to obtain almost uniform electric field (Section 3.2), the signal variation can be minimized by changing the Accordion pitch or the LAr gap. For the optimized set of geometrical parameters chosen for the present prototype, the liquid argon thickness as a function of the x position is shown in Fig.4. The maximum variations ($\pm$ 5%) are seen by a minimum ionizing particle hitting the calorimeter front face at normal incidence. For a high energy shower a smoother response is expected. A comparison with the experimental results is presented in Section 4.2.2.

The fast readout also contributes to the uniformity of the response. In fact, when the electron drift current is integrated over the whole drift time t_d, the charge deposited in a symmetric gap with a collecting electrode in the centre is effectively weighted by a triangular function with zero weight close to the electrode and maximum far from it. For $t_p << t_d$ this weight is smaller but uniform over the gap [4]. Similar considerations show that the sensitivity to mechanical imperfections like widening of the distance between converter plates, is also reduced in case of fast readout.

3.1 The construction

In order to reach good uniformity in the response, the mechanics of the detector has to be built with rather strict tolerances. For this purpose an adequate fabrication procedure for the Pb–stainless steel sandwiches was developed at CERN in collaboration with a specialized firm [4]. Gluing was done using "prepregs" layers, which can be manipulated with their protective films for a few hours at room temperature. In a first step one side of the prepreg was put in contact with the stainless steel plate. The lead foil was then sandwiched in between two such layers and the package formed in this way was bent into the desired accordion shape using a tool developed at CERN for this purpose [2]. In a second step the remaining protective films were removed and the stainless steel was put in contact with the Pb foil. Using a specially constructed mould the sandwich was then heated to 120^0 C for two hours under a pressure of 50 N/cm^2 for final gluing.

3.2 The electrodes

The readout electrodes consist of two foils of double–sided copper clad Kapton glued together. Each plate has two layers of 35μm copper separated by 25 μm Kapton

[3]The adopted reference system has the z axis along the incident beam direction, the y axis along the vertical and the x axis along the horizontal direction oriented as shown in Fig. 2.

[4]Stesalit AG Zulwill, Switzerland.

and by glue. The overall thickness of the circuit is about 400 μm.

The two inner conductive layers, which are connected together, collect by capacitive coupling the fast signal from the electrons drifting in the gap. They are DC coupled to the preamplifier input (see Section 3.3).

The two outer layers are at high voltage. In order to protect the preamplifiers from accidental sparking, these layers consist of alternating regions of copper and special resistive coating [5].

The conductive layers are cut into 15 longitudinal strips 24 mm wide separated by 1 mm gaps. The electrode circuits were produced flat and then bent, using the tool mentioned above, with the same pitch and radius of curvature (3 mm) as the converter plates.

With such an electrode shape the electric field in the detector is not uniform. The radius of curvature of 3 mm was chosen so that the electric field nowhere exceeds the value it has in the flat sections by more than 10%. The effect of this non uniformity on the calorimeter response is discussed in Section 4.2.1.

3.3 The readout electronics

The prototype has a twofold longitudinal segmentation with connections to the readout on the front and back faces. Three strips adjacent in x are connected together to form a cell of 2.5 cm (in y)$\times$2.7 cm (in x). A total of 336 such cells were equipped for the beam test measurements.

The connection of three strips to form a cell is achieved by using a motherboard which holds the preamplifiers (8 per board). Each strip is in fact a transmission line of 15 Ω impedance. If considered as a lumped load, the 3 strips in parallel represent a capacitance of 400 pF and an inductance of 10 nH. Therefore a rise time of the circuit as short as $\tau = 4 \cdot \sqrt{LC} = 8\ ns$ can be reached provided that the preamplifier input impedance is low enough to satisfy the critical damping condition, i.e. $R_{in} = 4\sqrt{LC}/2C = 10\ \Omega$ [3]. The charge transfer speed in this test was limited by the fact that the available preamplifiers had R_{in}=20–30 Ω. Smaller values of R_{in} are desirable and foreseen for future tests [2].

Two types of charge sensitive preamplifiers have been used. One is based on the design developed for the Helios experiment [5] and consists of a hybrid circuit with input silicon J–FETs[6]. In order to allow electromagnetic shower studies at CERN SPS energies of up to 150 GeV, a feedback capacitance as large as 22 pF was used. In the present situation without input–matching transformers, a large FET at the input would be suitable, both for noise figure and rise time. However a large enough quantity of these elements with good perfomances was not available in time for the beam test described here and a smaller input transistor (20 pF) was used instead. In these conditions the input resistance at LAr temperature is about 25 Ω.

About 20% of the prototype channels were equipped with preamplifers based on GaAs MESFETs already adopted for cryogenic particle detectors and modified for the present application [6]. These preamplifiers use ten MESFETs in parallel reaching an input capacitance of 80 pF. The feedback network consists of a 22 pF

[5] 10$k\Omega$/square product RS15114 from ESL SNC (USA).

[6] Interfet, Dallas (USA).

capacitor in parallel with a 330 $k\Omega$ resistor. The Equivalent Noise Charge at 77^0K for a detector capacity of 400 pF is about 10^4 electrons rms for bipolar shaping with 100 ns peaking time. The input resistance is 20 Ω.

For both, the Si and the GaAs preamplifiers, the power dissipation is about 70 mW.

The readout chain included also an intermediate amplifier installed on the cryostat cover, a bipolar shaper with $t_p(\delta) \simeq 100$ ns and a 12–bit peak sensing Analog–to–Digital Converter (ADC Lecroy 2281). The latter two were located in the counting room.

The noise of the electronic chain was determined by measuring the fluctuation of the ADC pedestals. With the energy scale determined as described in the next section it is about 3.6 MeV/cell (4.8 MeV/cell) when the GaAs (Si) preamplifers are used. The total noise due to n cells has been measured to scale incoherently as $\sqrt{n}$.

3.4 The calibration system

Good performances of any calorimeter strongly rely on accurate calibrations which directly affect the uniformity of response and the energy resolution of the detector. Calibration becomes a serious practical problem when a large volume detector with high granularity (order of 10^5 channels), as foreseen for experiments at the LHC and SSC, is envisaged.

One of the merits of calorimeters based on the ionization chamber technique is that they can be calibrated relatively easily and fast. All channels are equalized with a purely electronic method by injecting a known charge at one end of the readout chain, whereas the absolute energy scale, determined locally with a particle beam, can be extended to the whole calorimeter. This procedure relies on the homogeneity of the liquid inside the detector and on the assumption that tight mechanical tolerances can be maintained throughout the calorimeter.

In particular if one aims at a small constant term ($\leq 1\%$) in the energy resolution of the electromagnetic section a very accurate and stable calibration system is needed. The one adopted for the prototype described here used a set of precise test capacitors of about 22 pF measured to an accuracy of 0.2 pF ($\sim 1\%$). These capacitors were installed on vertical boards (15 per board) mounted directly on the calorimeter front and back faces ahead of the preamplifier cards, i.e. at the entrance of the electronic chain.

The calibration procedure consisted of injecting a sequence of step pulses in the range $0 \rightarrow 1$ V into each test capacitor and of reading the output of the corresponding ADC. In this way a conversion factor from ADC counts to pC was determined for each channel. The pulse generator was a Digital–to–Analog Converter (DAC) module that delivered step signals uniform to within $\pm$ 0.25%. A proper RC network was used to obtain a quasi–triangular signal, thus emulating the shape of the current produced by a particle traversing the detector. In order to enable cross–talk studies, only one channel out of three, both in the vertical and horizontal directions, was pulsed at a given time. This procedure was repeated typically two times per day during data taking.

The absolute energy scale was fixed using a 122 GeV/c incident electron beam by imposing that the mean signal released in the calorimeter was equal to the effective beam energy. This gives a calibration factor of $\sim 0.4pC$ per incident GeV and a sensitivity of the electronic chain of about 18 MeV per ADC count.

4 Test Beam Results

4.1 The experimental set-up

The results described in this paper were obtained during one week of parasitic run by exposing the prototype to electron and muon beams in the H6 line of the CERN SPS. Electron data were taken in the energy range 30 to 150 GeV/c. A secondary (tertiary) electron beam was available above (below) 90 GeV/c. Above 90 GeV/c electrons were well separated from pions by synchrotron radiation energy loss in traversing a set of bending magnets. Below 90 GeV/c the beam was unseparated with a 30% concentration of electrons. Pions in the beam were recognized by means of a hadronic calorimeter installed behind the test module (see below). Muons were provided by particle decay from a secondary 150 GeV/c pion beam. The typical particle flux was a few kHz over a beam spot of 2 $cm \times 2$ cm.

The direction of the incident particles was determined by means of two proportional wire chambers (PWC) placed 2.5 m and 7.5 m upstream of the calorimeter. Each chamber provided the particle position in the x–y plane with a resolution of about 310 μm for each view. Discrimination against multiple hits was also possible using the x coordinate. The resulting accuracy on the particle impact point on the calorimeter was 506 ± 10 μm.

The chamber readout was triggered, as the calorimeter, by the coincidence of two 10 $cm \times 10$ cm hodoscopes (S1-S2) and of one 2 $cm \times 2$ cm counter (S3) placed along the last 7 m of the beam line. Muons were identified by an additional 30 $cm \times 30$ cm hodoscope (S5) located downstream of the calorimeter behind a 2 m thick iron absorber.

The test module was installed inside the cryostat of the Helios experiment and backed up by the Helios uranium-liquid argon sampling calorimeter [7]. This downstream calorimeter, 1.2 $m \times 1.2$ m area for about three interaction length thickness, was used to help in electron/pion discrimination and to collect the eventual leakage of electromagnetic showers from the two segments of the prototype. The cryostat vessel consisted of a cylindrical stainless steel container of 93 cm radius and 0.3 cm wall thickness followed by a vacuum gap of 2.7 cm and a 2 cm thick aluminium wall. It was mounted on a rail system which allowed horizontal movements perpendicular to the beam axis. The LAr contamination was monitored to be below the 1 ppm level.

4.2 Response to electrons

The response of the prototype to electromagnetic showers was studied with 29, 59, 89, 122 and 146 GeV/c incident electrons (momentum spread 0.2%) striking the calorimeter centre. The test module was also scanned 10 cm in the horizontal direction. In this first test the beam quality was degraded by the presence of about two

radiation lengths of material distributed over 40 m upstream of the calorimeter and belonging to other experiments running on the same beam line. The signals from the three upstream scintillating hodoscopes were therefore used in the offline analysis to reject events with more energy than expected for a single minimun ionizing particle.

The electromagnetic showers were reconstructed in each compartment of the calorimeter by adding the energy deposited in a matrix of contiguous cells around the readout channel with the highest signal. All of the particle energy is contained in a matrix of 7×7 cells while typically 2% (7%) of the signal is lost when the size is reduced to 5×5 (3×3) cells, which corresponds to an area of $13.6 \times 12.5\ cm^2$ ($8.1 \times 7.5\ cm^2$). All the results presented below refer to the case of 5×5 cell clustering. Similar numbers were obtained with the $3 \times$ 3 cell matrix, which is probably more suitable for physics at future hadron colliders.

4.2.1 Energy resolution

The energy spectrum for 122 GeV electrons is shown in Fig. 5. The non–Gaussian tail on the left side of the distribution is due to particles losing energy by bremsstrahlung in the material upstream of the calorimeter and yet surviving the beam hodoscope and chamber cuts. The magnitude of this effect depends on the tightness of the cuts and has been reproduced by a Monte Carlo simulation of the beam line setup. Therefore the energy spectra have been fitted with a Gaussian shape within -1σ and $+2\sigma$ around the maximum. At 122 GeV the energy resolution is 0.95% whith both, the 5×5 and the 3×3 cell cluster. No correction for an eventual small energy leakage in the hadronic calorimeter has been applied. The resolutions obtained with different beam energies are shown in Fig. 6 and fitted with a curve of the type

$$\frac{\sigma}{E} = \frac{k}{\sqrt{E}} + c$$

The result of the fit is

$$\frac{\sigma}{E} = \frac{10.0 \pm 0.6}{\sqrt{E}}\% + (0.0 \pm 0.1)\% \quad \text{or} \quad \frac{\sigma}{E} = \frac{10.1 \pm 0.4}{\sqrt{E}}\% \oplus (0.2 \pm 0.2)\%$$

where in the second case the two terms are added in quadrature. It can be seen that the contribution of the constant term c, which reflects the presence of systematic effects, is consistent with zero over a calorimeter area of $2\ cm \times 2\ cm$.

The dependence of the energy resolution on the intensity of the electric field has been investigated with a 122 GeV/c electron beam by varying the detector high voltage from 1200 V to 2500 V (Fig. 7). No deterioration of the resolution is visible at low voltage showing that the calorimeter response is not affected, at least over this HV range, by the inhomogeneity of the electric field along the Accordion folds. The operation point was chosen to be 2000 V ($\sim 10\ kV/cm$). At this value the response does not yet reach a plateau because the electron drift velocity is not completely saturated [8].

4.2.2 Uniformity of response

Signal uniformity and energy resolution are directly correlated. A locally good energy resolution could be worsened by the signal variations with the particle impact

point. In the Accordion calorimeter these variations might be produced by the complicated geometrical structure and in particular, as discussed in Section 3, by the rounded corners of the absorber plates.

Experimentally the local variation of response with particle impact point was studied by scanning a calorimeter cell in steps of 1 mm along both the horizontal and the vertical directions. The 122 GeV/c electron beam was used for this measurement. The results are shown in Fig. 8. Along x the response shows a threefold periodical structure which reflects the accordion geometry (each cell is made up of three interconnected adjacent strips). This behaviour is consistent with the prediction of a full shower Monte Carlo simulation [9] of the calorimeter also shown in the figure. The signal variation along this view is within $\pm 1\%$ from the mean with an rms of 0.4%. Some discrepancy between Monte Carlo and data can be attributed to mechanical imperfections in the prototype stacks and to a possible tilting of the test module with respect to the plane orthogonal to the beam direction. As expected the structure does not appear in y where the response is homogeneous (rms 0.1%).

Due to the smearing introduced by the signal variation as a function of the electron x position, the overall energy resolution measured over a region of 2 $cm \times$ 2 cm is slightly worse (about 10% worse at 122 GeV) than that which could be achieved for a fixed impact point.

Finally a 10 cm (four cells) horizontal scan with a 122 GeV/c electron beam has shown that the variation of the prototype response stays well within $\pm 1\%$.

4.2.3 Space resolution

The calorimeter information can also be used to reconstruct the impact point of the incident particle, which is determined as the energy weighted barycentre of the 5×5 cell cluster. The accuracy of this measurement can be quantified by looking at the deviation from the impact point reconstructed via the beam chambers (Fig. 9). In the horizontal view the width of the distribution is 690 ± 22 μm for 122 GeV/c electrons. After the PWC resolution of the impact point (± 506 μm) has been unfolded, the resulting calorimeter space resolution is 470 ± 24 μm. Only the first segment of the prototype was used for this measurement in order to avoid the spread introduced by a possible misalignment of the module with respect to the beam direction.

The dependence on the electron energy of the space resolution in x is shown in Fig. 10. The measured values can be fitted as

$$\sigma_x = \frac{(4.38 \pm 0.36)\ mm}{\sqrt{E}} + (0.07 \pm 0.04)\ mm$$

For a consistency check, the resolutions measured at different energies have been fitted without unfolding the beam chambers resolution. In this case a constant term of 544 ± 28 μm is obtained, which is consistent with the contribution expected from the PWC system.

Such good spatial resolution of the prototype along the horizontal view can be attributed to its peculiar geometry. Since the projected transverse dimension of the Accordion fold is equal to the cell size in x (about 2.7 cm), an incident ionizing particle will always give a signal shared by at least two neighboring channels, thus

improving the accuracy in the reconstruction of the barycentre. Along the vertical direction, on the other hand, the detector behaves like a conventional calorimeter. The spatial resolution depends on the impact point, namely it is better at the cell edge where the energy sharing between two adjacent channels is maximum. The different behaviour of the prototype along the two transverse axes is illustrated in Fig. 11, where the position of the incident 122 GeV/c electrons, as reconstructed by the calorimeter, is compared to the impact point determined by the beam chambers. The variation of the points density in these plots is due to the beam spot shape which did not illuminate uniformely the cell surface. In Fig. 11b the flattening of the distribution at the cell centre reflects the poor precision of the calorimeter measurement when most of the energy is contained in only one channel, whereas Fig. 11a demonstrates how the energy sharing between cells inherent to the Accordion structure results in a spatial resolution independent of impact point. Consequently the x coordinate of the impact point reconstructed by the calorimeter can be used directly without additional manipulation and therefore exploited for instance at the trigger level.

In the y direction the observed shape can be fitted with the form

$$y_{CALO} = a \cdot \tan\left(\frac{y_{PWC}}{b}\right) + c \quad \text{with} \quad a = 0.2 \quad b = 0.42 \quad c = 0.01$$

in cell units, which can then be used to correct the reconstructed calorimeter position as a function of the particle impact point. The y space resolution obtained after this correction and after unfolding the beam chambers resolution is $\sigma_y = 570 \pm 25\ \mu m$ at 122 GeV.

4.2.4 Lateral shower size

Although on the one hand the geometrical structure of the Accordion yields excellent spatial resolution in the horizontal direction, on the other hand it may artificially increase the observed lateral shower size along x with respect to that along y. A comparison of the shower width in the two coordinates is shown in Fig. 12. The width is defined as the second order moment of the energy distribution and is plotted in the figure as a function of the electron impact point on the test module. It can be seen that in general if the incident particle is close to the boundary between two channels the observed shower profile tends to be wider than at the cell centre because the maximum energy sharing. The effect of the Accordion structure along x is evident from the different shapes of the distributions in Fig. 12a and Fig. 12b. Typically for a given impact point the lateral shower size in x exceeds the width in y by about 2 mm (15-20% effect).

4.3 Response to muons

A few muon runs were taken in the test to study the response of the prototype to minimum ionizing particles.

To identify muons in the incident 150 GeV/c pion beam a coincidence between the upstream beam counters $S1$ and $S2$ and the "muon counter" $S5$ was required in the trigger. Data were taken with particles incident in the calorimeter region read

out by the GaAs preamplifiers. Since the signal produced by the incident muon is always shared by at least two channels adjacent in x, the energy released in the prototype was reconstructed in each compartment by adding the signals from the most energetic pair of neighboring cells along x. For nearly normal beam incidence, this 2×1 cell cluster in the $x \times y$ directions is adequate to contain all the energy deposited by a muon except when the particle position is closer than 2 mm to the boundary between two adjacent cells along the y direction. About 10% of the signal is lost in this case. These impact points were eliminated in the present analysis by applying a fiducial cut.

The total energy released by muons in the two compartments of the prototype is shown in Fig. 13. The same energy scale has been used as for electron data. This scale was determined with 122 GeV/c electrons as described in Section 3.4 and takes into account that only about 18% of the energy deposited by an incident electron is released as visible signal in the liquid argon. With this scale the most probable energy loss (1 mip) is 350 MeV. In Fig. 13 the tail of the spectrum is plotted up to ~ 2.6 mip.

The energy spectrum predicted by a detailed Monte Carlo simulation of the calorimeter geometry is also plotted in the figure. In the simulation the distribution of the muons position in the calorimeter reproduced the experimental situation. An identical clustering algorithm as in the data analysis was used to reconstruct the deposited energy and the same 2 mm fiducial cut at the y boundary between two cells was applied. The noise of the electronic chain was also included. The simulation took into account all the material preceding the prototype, such as the cryostat walls, whereas the charge collection mechanism in the calorimeter and the details of the beam line setup were not implemented. It can be seen that the Landau shape of the experimental distribution is well reproduced by the Monte Carlo.

With the present electronics the ratio of the muon peak to the total noise of the four cells forming the muon cluster is 48. This value is expected to reduce to about 5 with fast shapers ($t_p(\delta) \simeq 20\ ns$).

In Fig. 14 the muon impact point along x reconstructed by the calorimeter (in the same way as described for electrons) is compared to the position determined via the beam chambers information. A space accuracy of $1.75 \pm 0.05\ mm$ is achieved in the horizontal direction after unfolding the PWC resolution. This result is substantially better than that expected for a conventional pad detector of comparable cell size.

5 Conclusions and Future Prospects

A novel design for a liquid argon sampling calorimeter in which the electrode and converter plates have an accordion shape has been realized. This peculiar geometry allows for fast detector readout and for high granularity over large volumes while introducing minimal dead space. These features are among the essential requirements for operation at future hadron colliders.

A first short test of a small electromagnetic prototype has given very promising results on energy resolution ($10\%/\sqrt{\mathrm{E(GeV)}}$), spatial resolution ($4.4\ mm/\sqrt{\mathrm{E(GeV)}}$), and uniformity of response for electrons. The aim of future tests is to demonstrate that these performances remain unaffected when a fast electronic chain with a shaper

peaking time $t_p(\delta) \simeq 20\ ns$ is used.

The design, construction and test of electromagnetic and hadronic prototypes of larger size and with pointing geometry are also part of the forthcoming programmes of this R&D activity.

Acknowledgements

The construction of the calorimeter prototype within a very short time was only possible with the substantial contribution of the collaborating institutes technical staff. We deeply thank them for their support and in particular we thank L.Bonnefoy, K.Bussmann, M.Cighetti, G.Di Tore, G.Dubail, G.Dubois-Dauphin, A.Garagiola and B.Monticelli.

Financial support is acknowledged from the Institut National de Physique Nucléaire et de Physique des Particules to the Annecy and Orsay group and from the Istituto Nazionale di Fisica Nucleare to the Milano group.

References

[1] Large Hadron Collider Workshop, Aachen 4–9 October 1990, ECFA 90–133 and CERN 90–10, editors G.Jarlskog and D. Rein.

[2] B.Aubert et al. (RD3 Collaboration), " Liquid Argon Calorimetry with LHC–Performance Specifications", CERN/DRDC/90-31 (1990).

[3] V.Radeka and S.Rescia, Nucl. Inst. and Meth. A265(1988)228.

[4] C.Cerri et al., Nucl. Inst. and Meth. 227(1984)227.

[5] SSC Detector R&D at BNL, Editors B.Yu and V.Radeka, BNL 52244,1990.

[6] D.V.Camin et al., "Cryogenic Charge–Sensitive Preamplifiers for High Dynamic Range and Fast Speed of Response Using GaAs Technology", Proc. of IEEE Trans. on Nucl. Sci. 38 (2), 1991.

[7] D. Gilzinger et al., "The Helios Uranium–Liquid Argon Calorimeter", paper in preparation.

[8] E.Shibamura et al., Nucl. Inst. and Meth. 131(1975)249

[9] Geant 314, R.Brun et al. in Proc. of Large Hadron Collider Workshop, Aachen 4–9 October 1990, ECFA 90–133 and CERN 90–10, editors G.Jarlskog and D. Rein.

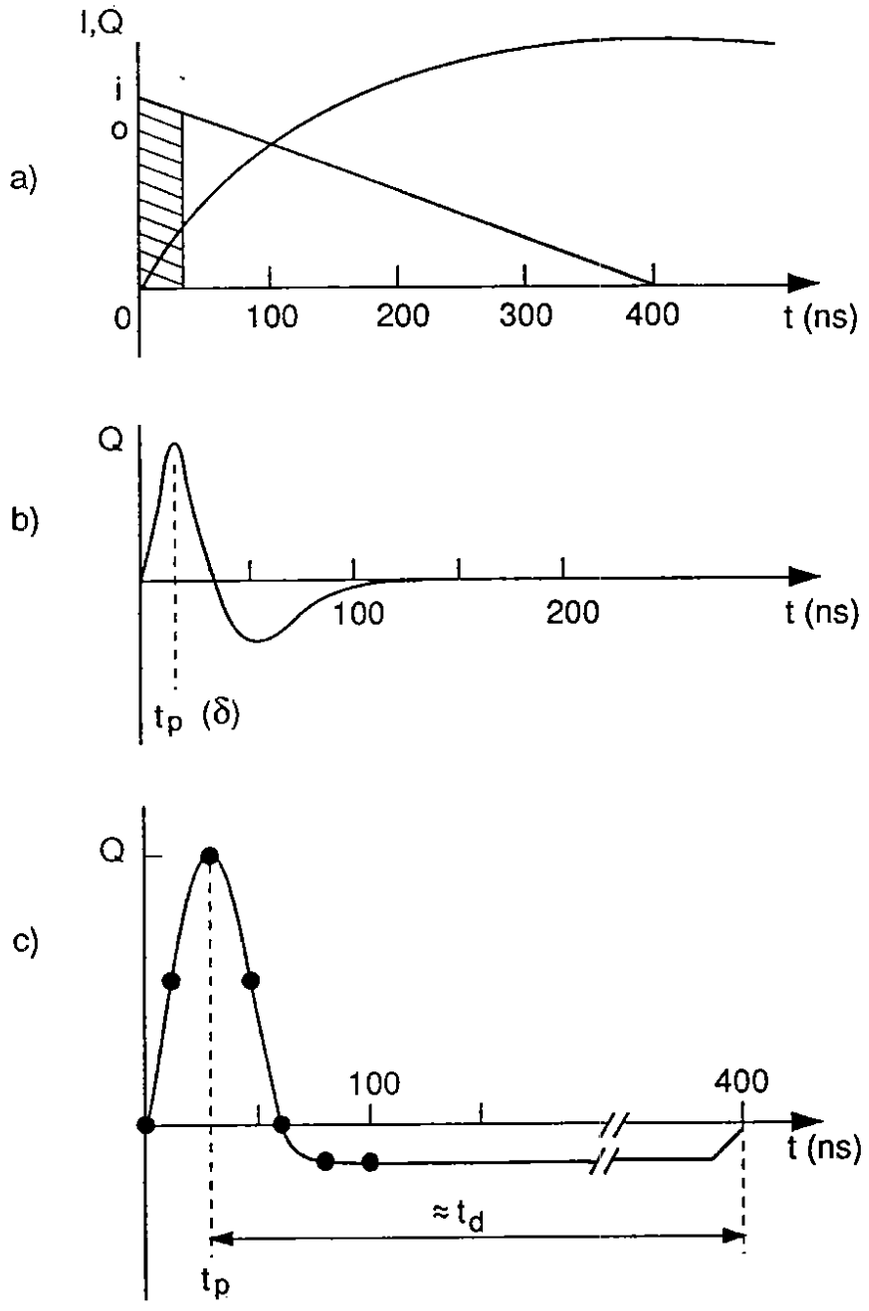

Figure 1: a) Drift current and integrated charge vs time for an ion chamber calorimeter. b) Response of a shaping amplifier to a short current pulse (δ). c) Response of a shaping amplifier to the current form shown in a). The dots indicate where the beam crossings (every 15 ns) would appear if $t_p(\delta) = 20\ ns$.

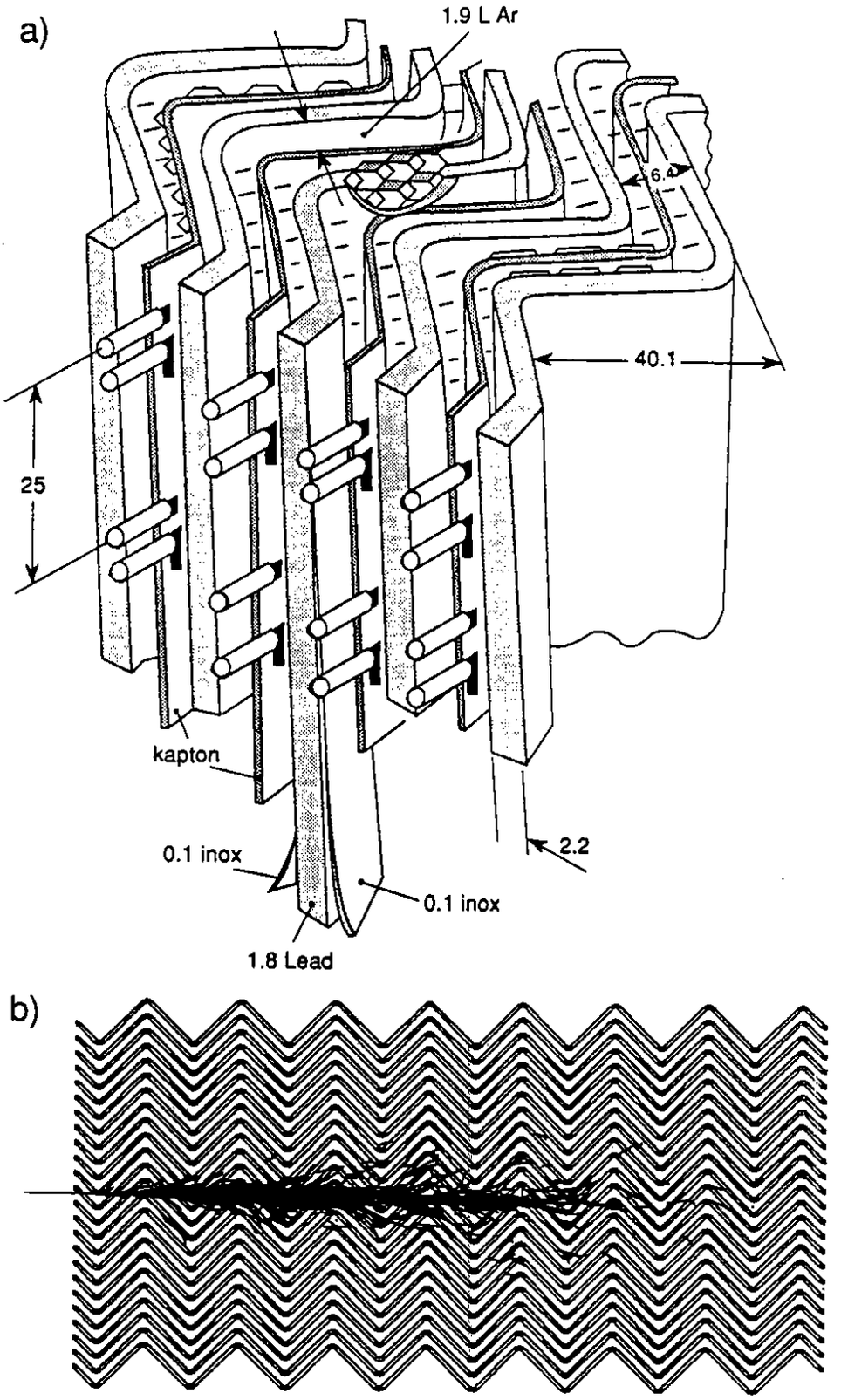

Figure 2: a) Artist's view of the Accordion calorimeter geometry. b) Development of a 40 GeV electron shower (Monte Carlo simulation). Only charged tracks above 10 MeV are shown.

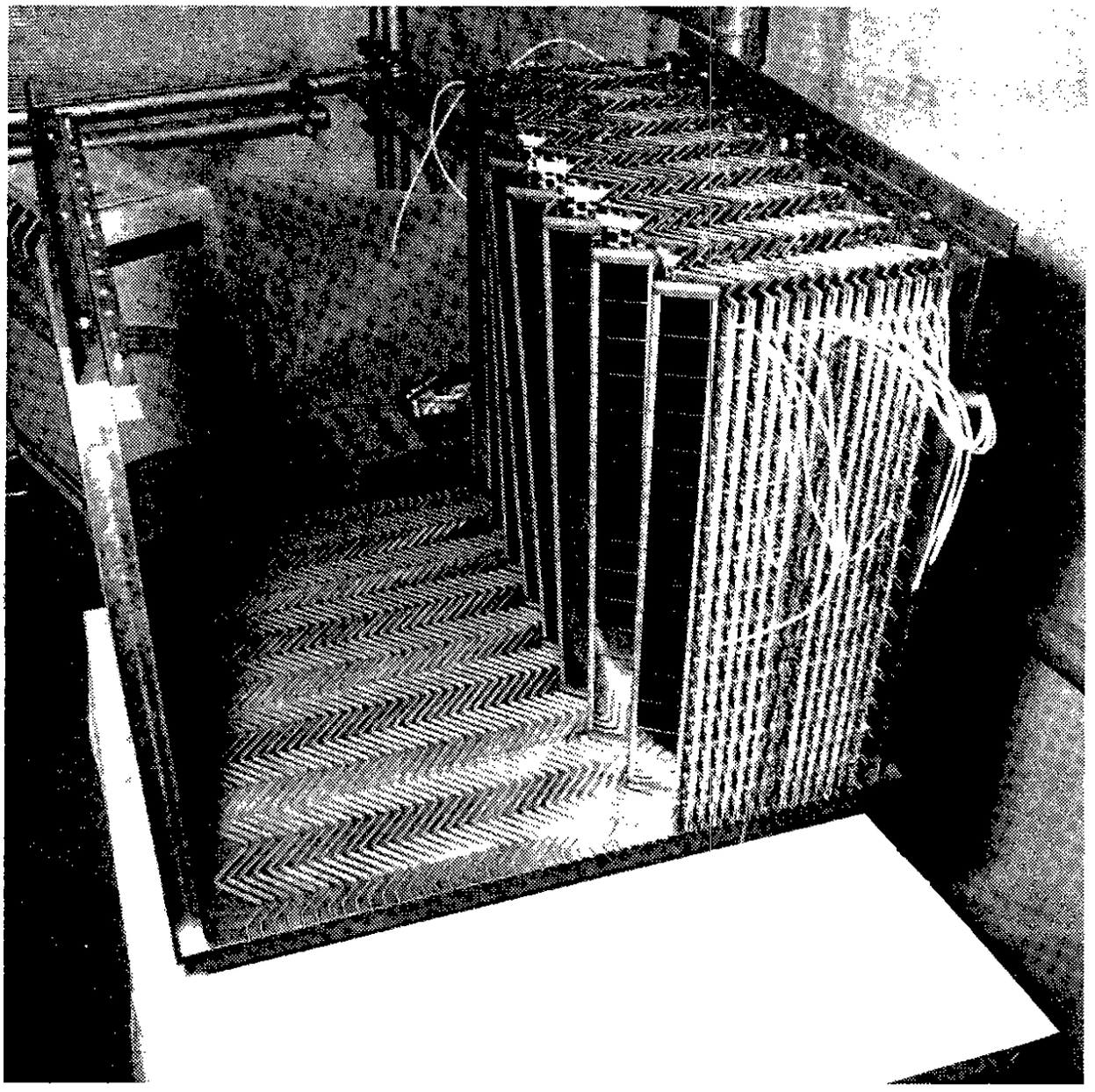

Figure 3: The Accordion test module during assembling inside its support box.

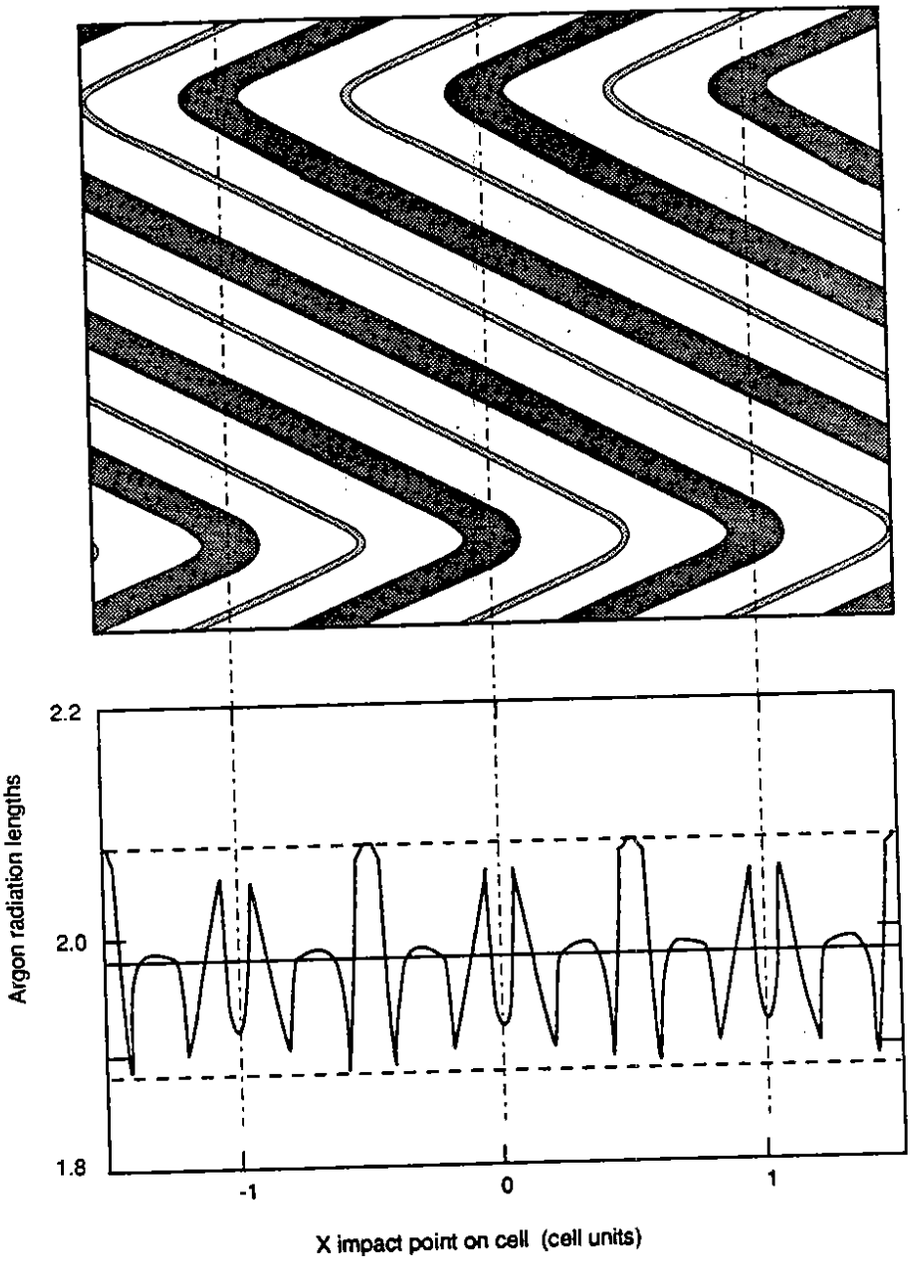

Figure 4: Total liquid argon thickness, in radiation lengths, as a function of the position along the x view of the prototype (Monte Carlo simulation). The dotted lines delimit a $\pm 5\%$ band around the mean value

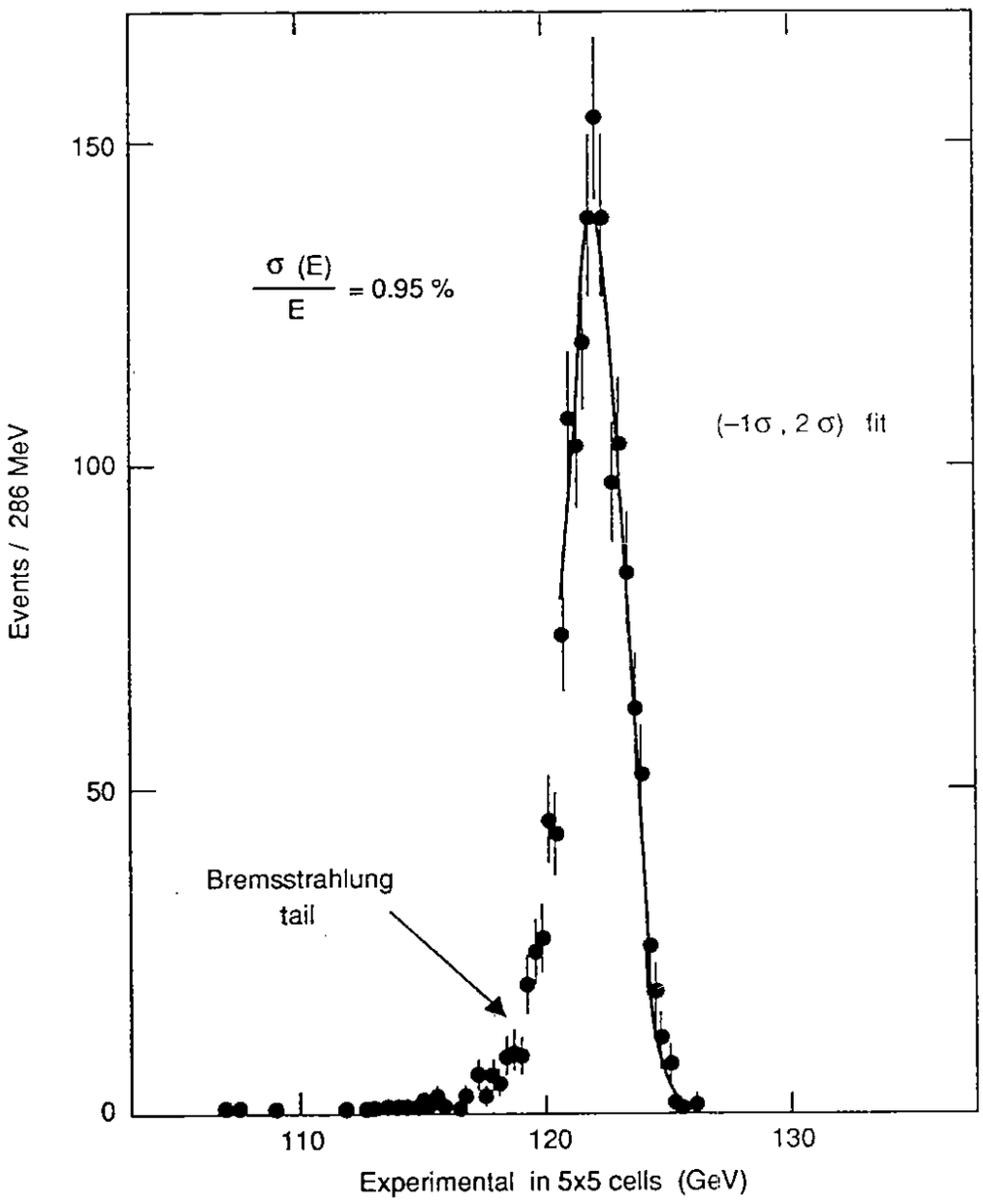

Figure 5: Energy reconstructed in the calorimeter for 122 GeV/c incident electrons. The solid line is a Gaussian fit (see text).

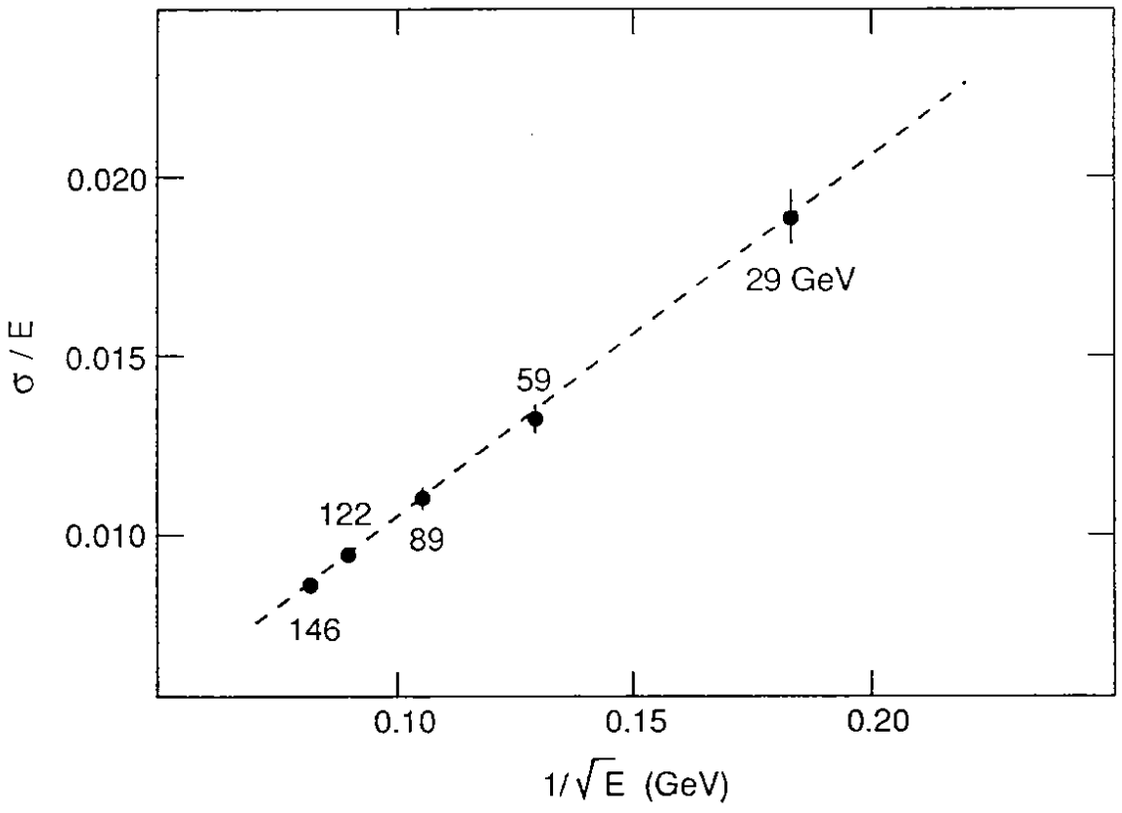

Figure 6: Energy resolution of the prototype at different electron energies. The dashed line is a linear fit to the experimental points.

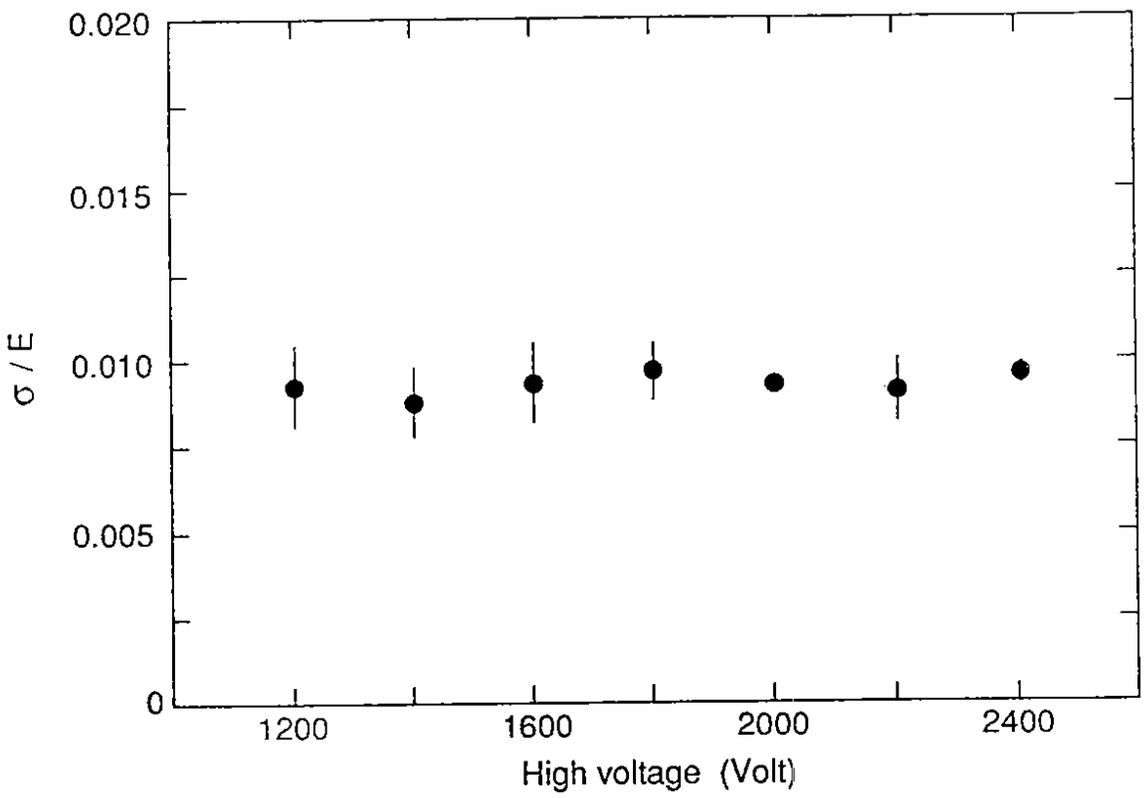

Figure 7: Energy resolution at 122 GeV as a function of the high voltage applied to the test module

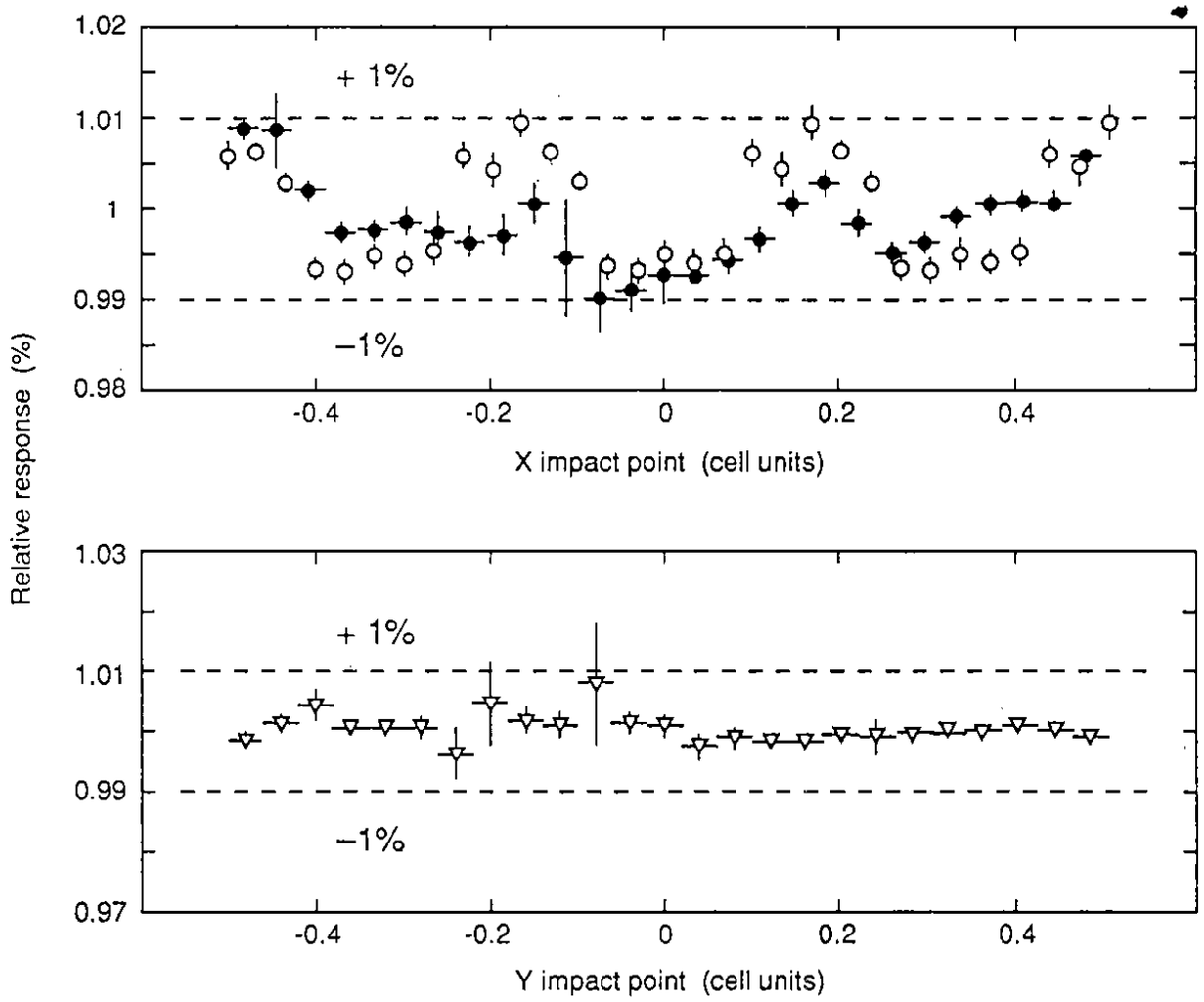

Figure 8: Relative variation of the calorimeter response over a cell as a function of the electron x (a) and y (b) position. Black symbols: experimental points. Open circles: prediction of a Monte Carlo simulation of the Accordion.
The dotted lines delimit the $\pm 1\%$ deviation from the mean

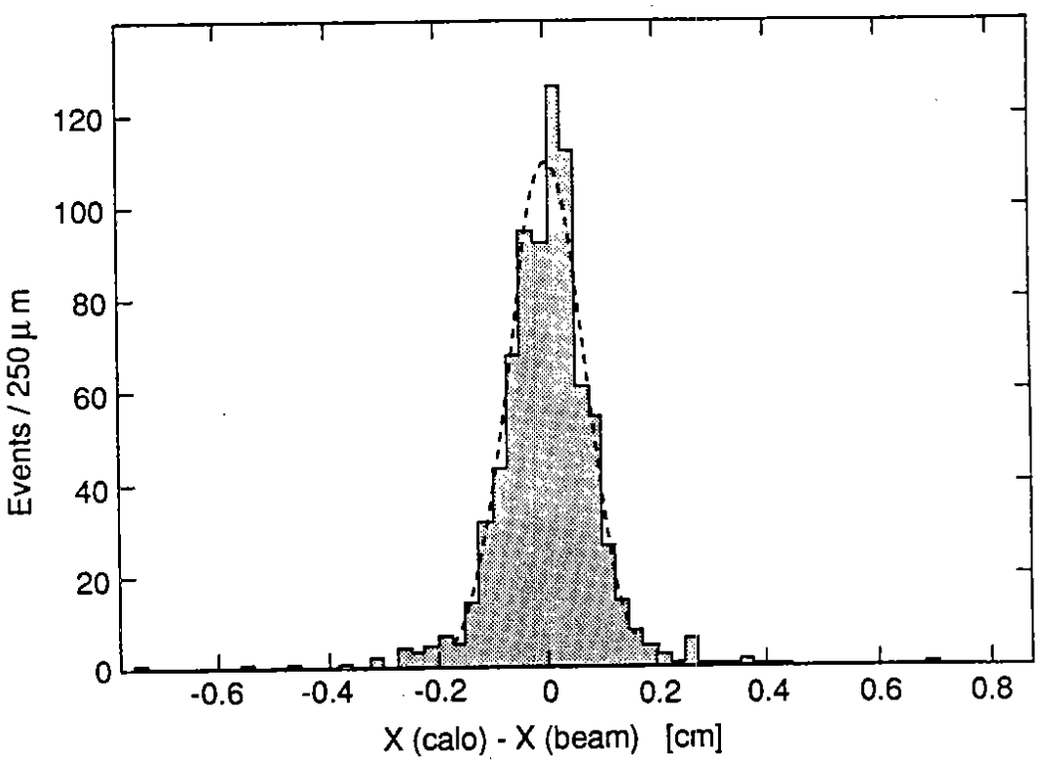

Figure 9: Difference between the x impact point as recontructed in the calorimeter and as determined by the beam chamber system for 122 GeV/c incident electrons. The dashed line is the Gaussian fit used to determine the space resolution

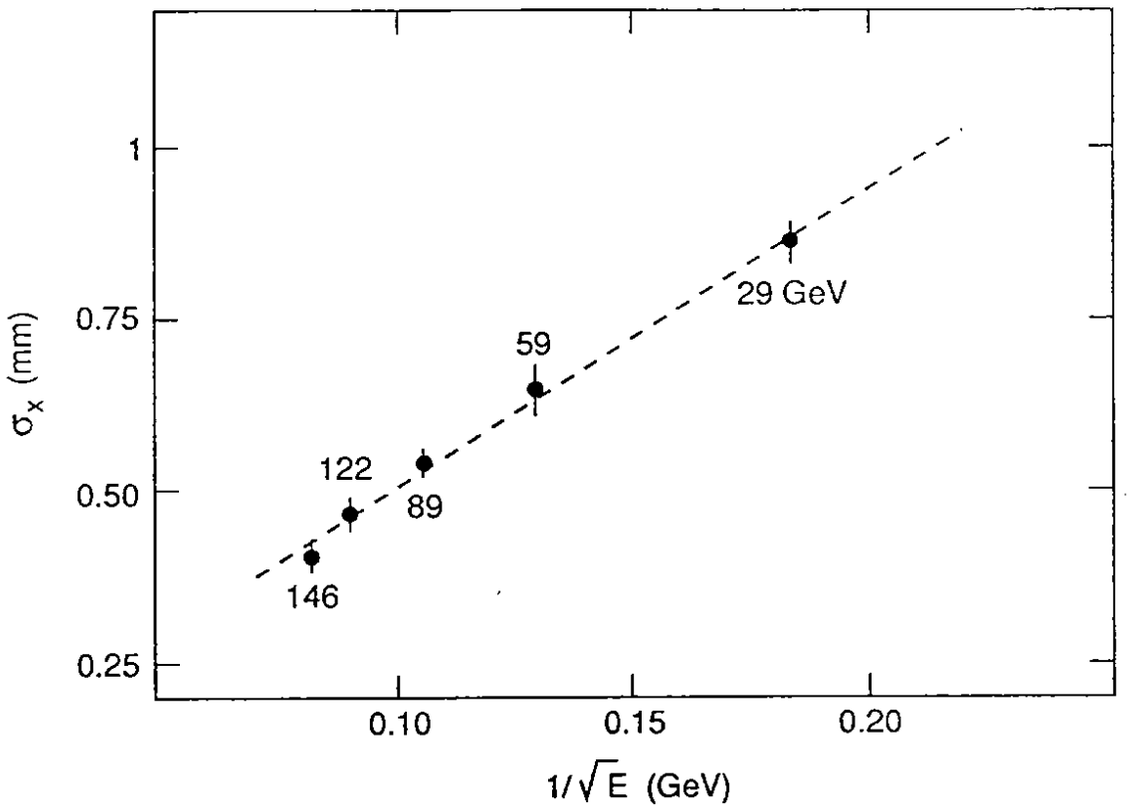

Figure 10: Space resolution of the prototype in the x view for different electron beam energies. The dashed line is a linear fit to the data points (see text).

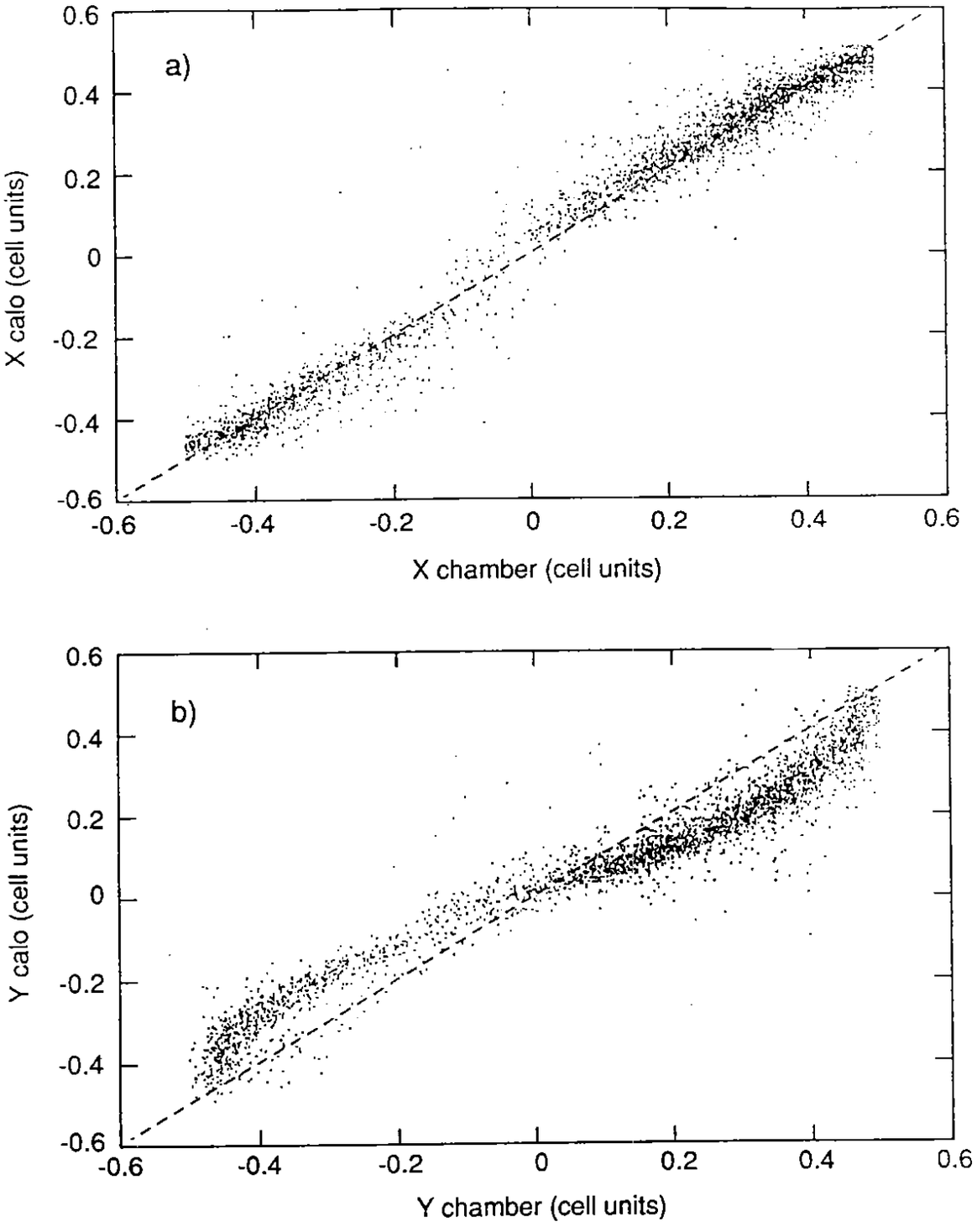

Figure 11: 122 GeV/c electron impact point as reconstructed by the calorimeter versus the position determined by the beam chamber system in the x (a) and y (b) view.

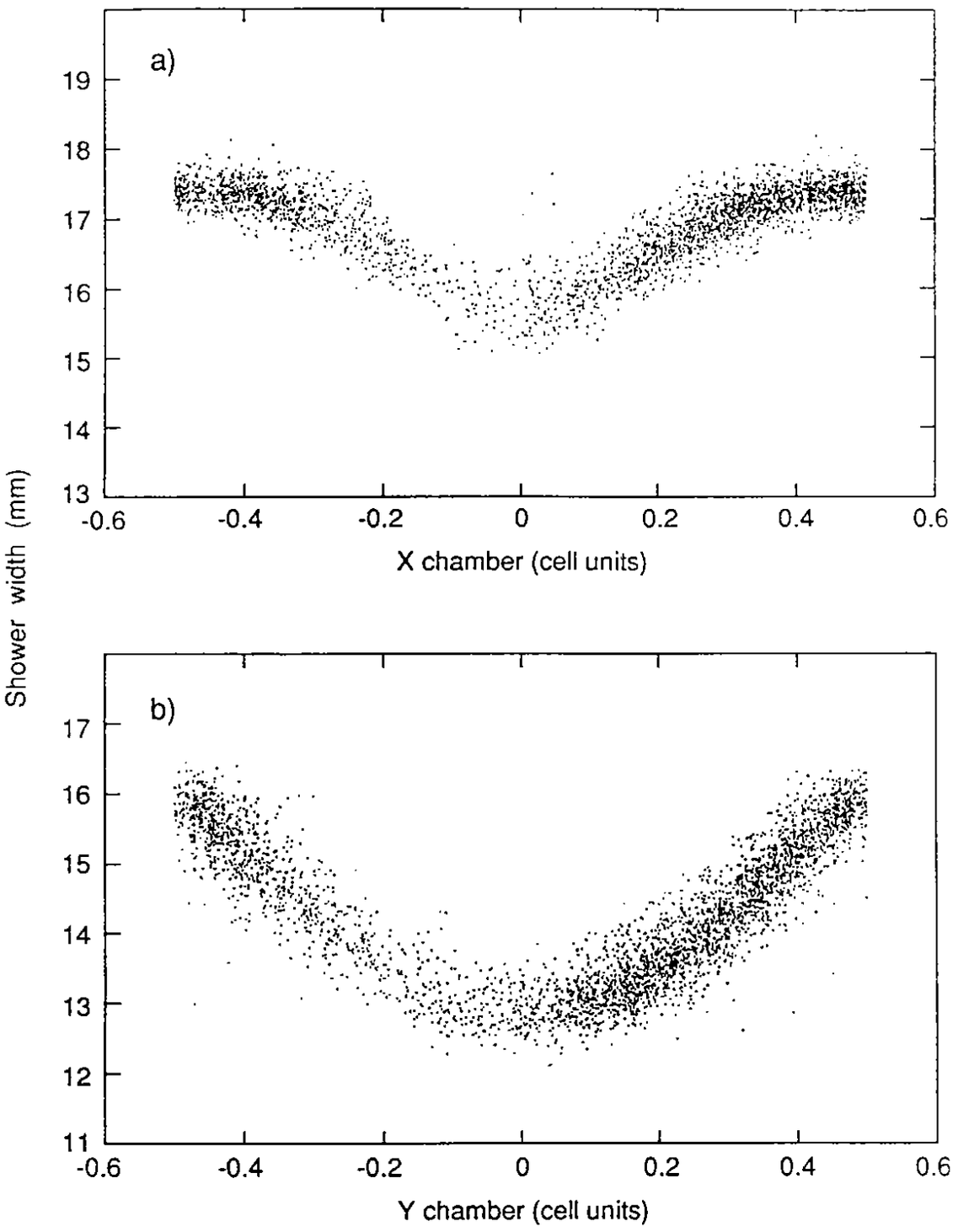

Figure 12: Lateral shower size in the x (a) and in the y (b) view for 122 GeV/c incident electrons as a function of the particle impact point on the prototype as determined by the beam chambers

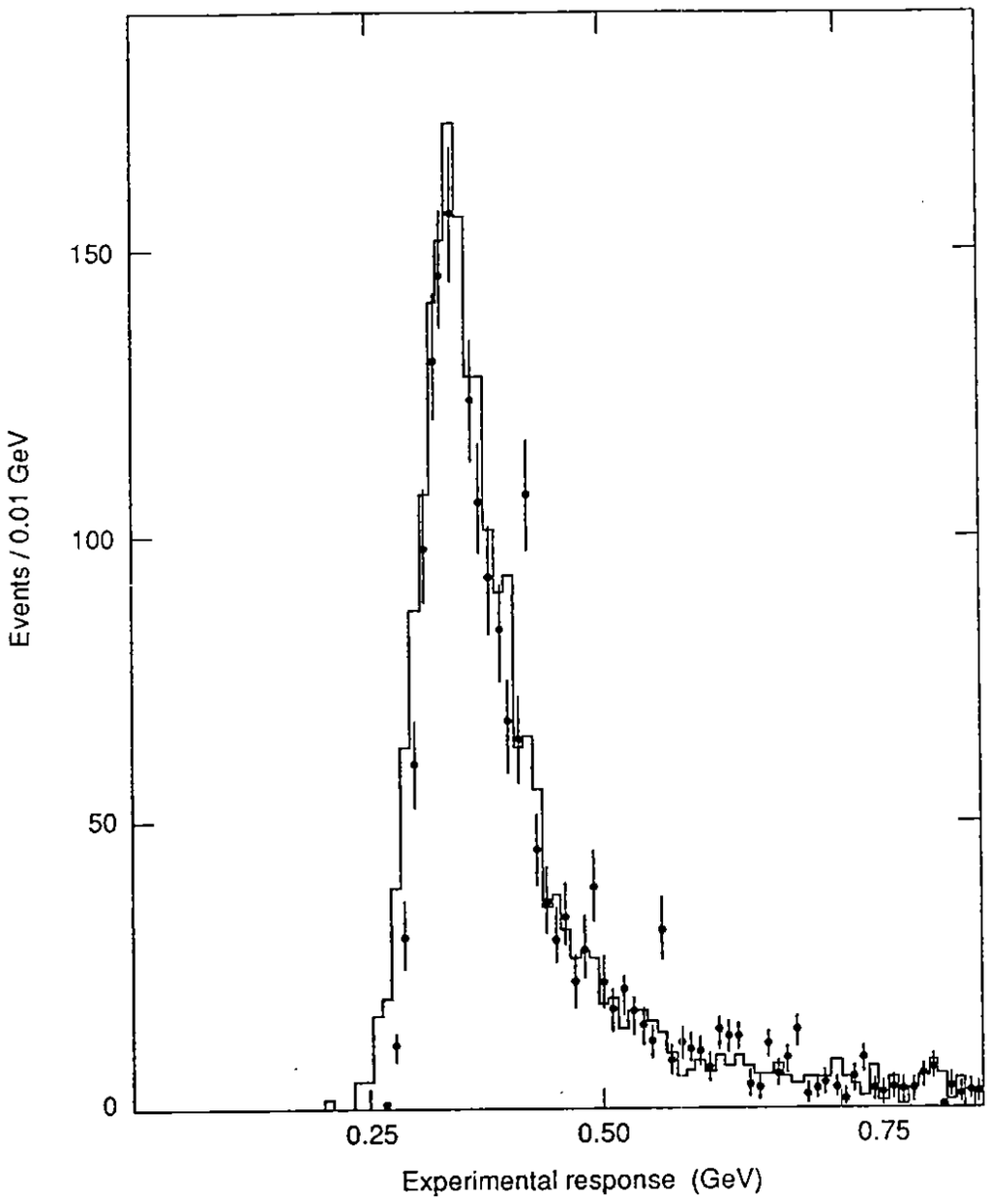

Figure 13: Energy deposited in the prototype by $\sim$ 100 GeV/c incident muons The distribution for the test beam data (full line) is compared to the prediction of a Monte Carlo simulation of the calorimeter (points with error bar).

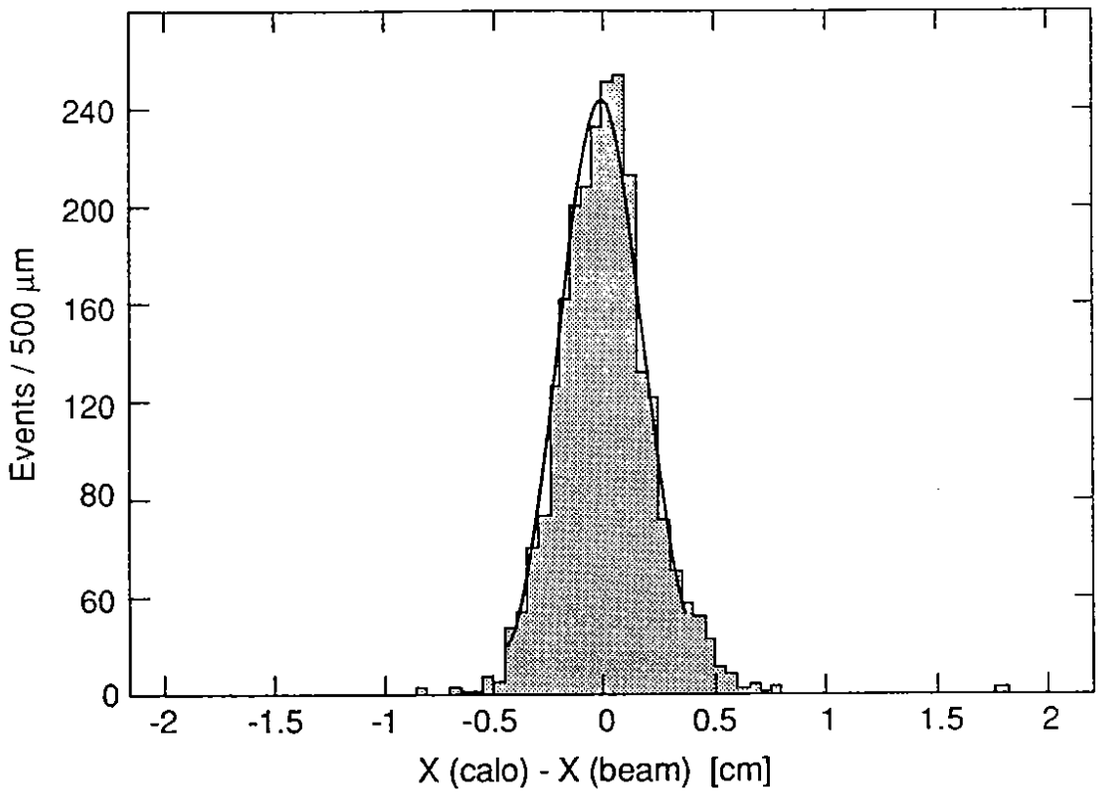

Figure 14: Difference between the muon impact point in the x view of the prototype as reconstructed in the calorimeter and as determined by the beam chambers system. The dashed line is the Gaussian fit used to determine the space resolution

Imprimé au CERN. Prix : 0.85 Fr.